Carbohydrate Polymers 121 (2015) 132–139

Contents lists available at ScienceDirect

Carbohydrate Polymers

journal homepage: www.elsevier.com/locate/carbpol

Synthesis and *in vitro* evaluation of a hyaluronic acid–quantum dots–melphalan conjugate

Haixing Xu[a,1], Jingbo He[b,1], Yu Zhang[a], Lihong Fan[c], Yaqiong Zhao[a], Tengfei Xu[a], Zhuang Nie[a], Xiangnan Li[a], Zhijun Huang[a], Bo Lu[a], Peihu Xu[a,*]

[a] *Department of Pharmaceutical Engineering, School of Chemistry, Chemical Engineering and Life Sciences, Wuhan University of Technology, Wuhan 430070 PR China*
[b] *The affiliated Baoan Hospital of Southern Medical University, Shenzhen 518101 PR China*
[c] *Department of Chemical Engineering, School of Chemistry, Chemical Engineering and Life Sciences, Wuhan University of Technology, Wuhan 430070 PR China*

ARTICLE INFO

Article history:
Received 9 November 2014
Received in revised form
15 December 2014
Accepted 24 December 2014
Available online 3 January 2015

Keywords:
Hyaluronic acid
Quantum dots
Melphalan
Drug delivery system

ABSTRACT

Polymer-drug conjugates have played an important role in improving tumor cell targeting and the selectivity of anticancer drugs. In this study, quantum dots and melphalan were attached to the backbone of hyaluronic acid to synthesize a polymer–drug conjugate. The physicochemical properties of the conjugate were characterized by FT-IR, XRD, ^{1}H NMR, UV-Vis spectra and DLS. The *in vitro* drug release profiles and cell evaluation were investigated. The results showed that the conjugate was synthesized and self-assembled into nanoparticles with a diameter of 115 ± 2.3 nm. The conjugate had a pH-sensitive drug controlled release property. It was an ideal receptor-mediated delivery system and can be internalized into the human breast cancer cell. It had a better inhibition effect on human breast cancer cell and a poorer inhibition effect on normal breast cell than melphalan. These results supported that the conjugate would be a promising candidate for cancer therapy.

1. Introduction

The increasing worldwide prevalence of cancer has made the cancer therapy one of the most intensively investigated targets in recent years. Great efforts have been made to improve therapeutic options (Goodarzi, Varshochian, Kamalinia, & Atyabi, 2013). The most considerable challenges facing effective cancer therapy are the systemic toxicity of cytotoxic drugs due to their nonspecific property, their lack of tumor localizing, and an even distribution throughout the whole body. Besides, short half-lives of anticancer drugs in blood circulation and their undesirable pharmacokinetic behavior are among other drawbacks which are present in the way of cancer treatment. All these negative effects have limited the clinical application of most of the anticancer drugs. Hence, there has been an eager quest to develop safe and efficient drug carriers which can deliver anticancer drugs exclusively to the targeting site without provoking adverse reactions in cancer therapy. Consequently, the conjugation of low molecular weight (MW) anticancer drugs to polymer carriers was commenced to form a polymer–drug conjugate which generally enhances the distribution of anticancer drug molecule (Shen, Li, Tu, & Zhu, 2009). The main advantages of polymer–drug conjugates include (Khandare & Minko, 2006; Majoros, Thomas, Mehta, & Baker, 2005; Moghimi, Hunter, & Murry, 2005; Patri, Majoros, & Baker, 2002): (1) an increase in water solubility of low soluble or insoluble drugs, and therefore, enhancement of the drug bioavailability; (2) protection of the drugs from deactivation and preservation of their activities during circulation; (3) a reduction in antigenic activity of the drug leading to a less pronounced immunological body response; and (4) most importantly, the ability to provide active targeting of the drug specifically to the site of its action.

Active targeting polymer–drug delivery systems have been investigated in recent years. These delivery systems recognize their targets by localization in tumors *via* conjugation to a chemical moiety with an affinity for an overexpressed/unique tumor cell marker (*i.e.* CD44 receptor, folic acid receptor, monoclonal antibody, *etc.*), or by triggering the release of anticancer drug from an environment-responsive carrier using a local stimulus (*i.e.* enzyme, pH, temperature, *etc.*) (Carole, Guy, Corinne, & Thierry, 2012). Among them polysaccharide-based systems have gained increasing attention due to their promising physicochemical and biological

* Corresponding author. Tel.: +86 02787749300.
E-mail address: xhx040328@whut.edu.cn (P. Xu).
[1] These authors contributed equally.

http://dx.doi.org/10.1016/j.carbpol.2014.12.057
0144-8617/

characteristics and simplicity of chemical reactions required for specific modifications (Carole, Guy, Corinne, & Thierry, 2011). Hyaluronic acid (HA) is a naturally-derived linear non-sulfated glycosaminoglycan polysaccharide, and a major constituent of the natural extracellular matrix (Laura, Marco, & Luisa, 2014). HA is naturally degraded in the organisms by a complex enzymatic mechanism involving hyaluronidase and HA cell internalization by CD44 cell surface receptors (Aruffo, Stamenkovic, Melnick, Underhill, & Seed, 1990; Jedrzejas & Stern, 2005). The hyaluronidase in tumor site is an acid-sensitive activity profile enzyme (Girish & Kemparaju, 2007). Recently, the use of HA as a drug carrier and a ligand to form conjugate has attracted much attention in active targeting drug delivery systems because of its ability to specifically bind to various cancer cells that overexpress CD44 receptors (Akima et al., 1996; Taetz et al., 2009; Sonia, Ana, & Carmen, 2011). The drugs are released once the covalent bonds are cleaved by intracellular hyaluronidase in the organisms, ideally at the specific target sites (Luo & Prestwich, 1999; Luo, Ziebell, & Prestwich, 2000; Pouyani & Prestwich, 1994; Xin, Wang, & Xiang, 2010).

Quantum dots (QDs) have been widely used owing to their interesting photophysical properties (Hridyesh, Rohit, & Dutta, 2013). These attributes make QDs superior fluorescent probes to organic fluorescent dyes and proteins for *in vitro* and *in vivo* biomedical imaging (Hauck, Anderson, Fischer, Newbigging, & Chan, 2010; Li, Duan, & Jing, 2011; Wang & Chen, 2011; Zhao, Liu, & Li, 2010). During the past years, CdTe and CdSe nanocrystals have become the most prominent QDs in area of life science, which have been widely used in cellular labeling and *in vivo* long-term fluorescence imaging (Hridyesh et al., 2013).

Melphalan (MEL), also known as l-phenylalanine mustard, is a potent anticancer drug and has been extensively utilized as a chemotherapeutic agent (Baracu, Balaban, & Wilman, 1990; Hansson, Lewensohn, Ringborg, & Nilsson, 1987). However, MEL is highly reactive, which can easily react with other cellular components including proteins and nucleic acids, resulting in the loss of therapeutic activity and the provocation of many undesired side effects such as bone marrow toxicity and genotoxicity (Li et al., 2014; Lu et al., 2013; Maze et al., 1996; Suzukake, Vistica, & Vistica, 1983). Moreover, it is water insoluble which leads to a very low bioavailability (Fermeglia, Ferrone, Lodi, & Pricl, 2003) In this study, a HA–QDs–MEL conjugate was developed to self-assemble nanoparticles for breast tumor treatment (Fig. 1). As expected, it has a promising active targeting ability to breast tumor and improved bioavailability. The results demonstrated that the conjugate had an ideal *in vitro* drug release, cytotoxicity properties, and cellular uptake characteristics, suggesting its potential as a future anticancer drug.

2. Materials and methods

2.1. Materials

Melphalan and hyaluronic acid (MW = 1,000,000) were purchased from Sigma–Aldrich. $NaHB_4$, Tellurium powder, $CdCl_2$ and L-cysteine were purchased from Sinopharm Chemical Reagent Co., Ltd., Shanghai, China. All other chemicals used were of analytical reagent grade. Double-deionized water was used throughout the experiment.

2.2. Synthesis of HA–QDs–MEL conjugate

37.8 mg of $NaHB_4$ and 63.8 mg of tellurium powder (2:1, molar ratio) were dissolved in 6 mL of deionized water and stirred at room temperature in darkness with N_2-saturated to prepare NaHTe solution until the color of the solution became to black. Then 114.2 mg of $CdCl_2$ and 90.87 mg of L-cysteine (1:1.5, molar ratio) were dissolved in 40 mL of deionized water in a 100 mL three-neck flask and the solution was alkalized to pH = 8.0 with 0.5 mol/L aqueous NaOH solution. Subsequently a certain amount of fresh NaHTe solution was added and saturated by N_2 for 30 min then 1 mL of Na_2S in water (7.5 mmol/L) was added and the mixture was refluxed to afford L-Cys-CdTe/CdS QDs solution.

100 mg of HA was dissolved in 100 mL of PBS (pH = 6.8) with 200 mg of EDC and 30 mg of NHS. After 30 min, 5 mL of L-Cys-CdTe/CdS QDs solution was added. After another 6 h, the solution was dialyzed (MW cut-off = 3000–5000 Da) and lyophilized, providing HA–QDs powder.

648 mg of Benzyl alcohol (BA) and 36 mg of $SOCl_2$ were mixed with vigorous stirring in ice bath, and 64.4 mg of MEL was added for esterification. Then the reaction mixture was concentrated and the residue was recrystallized from CH_3OH and ether to give a white powder (BA-MEL). The above HA–QDs were then dissolved in 50 mL of PBS with EDC and NHS. After 4 h, 60 mg of BA-MEL was added into the reaction mixture and stirred for 24 h. Then the reaction solution was dialyzed (MW cutoff = 3000–5000 Da) in double-distilled water and lyophilized. The HA–QDs–MEL conjugate was obtained upon removal of the methyl ester group by hydrogenolysis over palladium-charcoal.

2.3. Characterization

The Fourier transform-infrared (FT-IR) spectra were obtained and analyzed by a Flourier transform-infrared spectrometer (Nexus, Thermo Nicolet, USA) and the proton nuclear magnetic resonance (^{1}H NMR) spectra were recorded on an Inova 600 spectrometer (Varian, USA). HA–QDs–MEL was also characterized by ultraviolet–visible (UV–vis) spectroscopy (UV-2600, Shimadzu, Japan). The average hydrodynamic diameters and Zeta potential of HA–QDs–MEL nanoparticles (1 mg/mL) were measured by dynamic light scattering (DLS) using a Zeta sizer (Nano-ZS SDSB-10032; Malvern, UK). The experiment/test was carried out at 25 °C, and repeated three times.

2.4. In vitro drug release study

The drug release experiments were carried out at 37 ± 0.5 °C. Briefly, 5 mg of HA–QDs–MEL was dissolved in 50 mL of phosphate buffer solution (PBS) with 150 U/mL hyaluronidase and dialyzed in dialysis bags (MW cut-off = 12,000 Da) (Shan et al., 2012). Three buffer solutions with pH = 7.4, pH = 7.0, and pH = 5.8 were employed to simulate the pH values of microenvironments in blood vessels and tumor tissues, respectively. The dialysis bags were sealed at both ends with clips and placed into the medium with the same pH values of those in dialysis bags. At appropriate time intervals, aliquots of 1 mL medium were withdrawn and fresh equal volumes of PBS were added to the medium. Samples were analyzed by a Waters liquid chromatographic system (Waters 1525, USA) with a UV detector (SPD-10A, Japan) operated at 260 nm. A Waters ODS C18 column (4.6 × 150 mm, 5 μm particle size) was used at 30 °C. The mobile phase was a mixture of methanol, deionized water, and acetic acid (49:49:2, v/v/v). The injection volume was 10 μL, and the flow rate was 1.0 mL/min. The accumulative release rate % (Q%) was calculated by the following the formula,

$$Q\% = \frac{V_0 C_n + V(C_0 + C_1 + C_2 + \cdots + C_{n-1})}{m_0} \times 100\% \quad (1)$$

where V_0 stands for the total volume of the release medium, C_n (mg/L) is the concentration of the sample withdrawn at the interval of T_n, V is the volume of the sample withdrawn at the interval of T_i, C_i (mg/L) is the concentration of the sample withdrawn at the interval

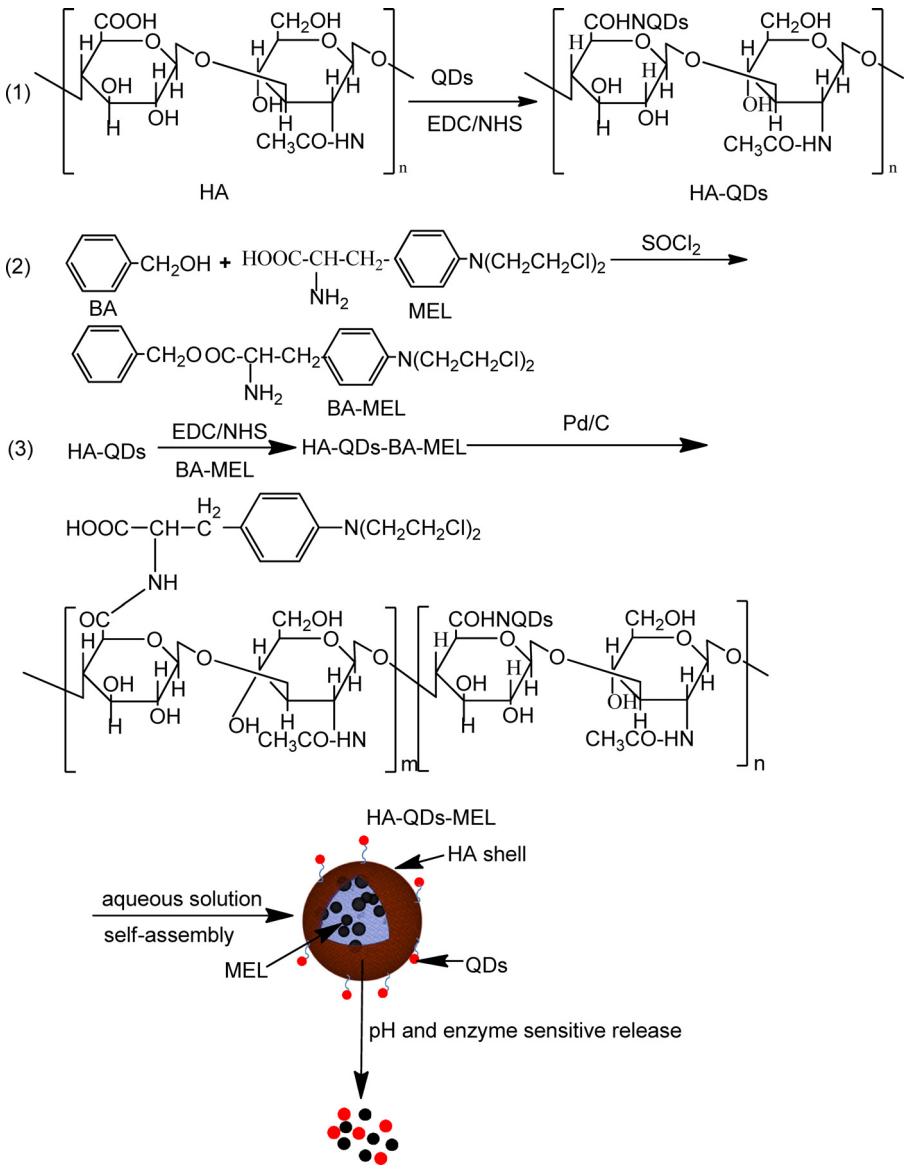

Fig. 1. The synthesis of HA–QDs–MEL and the illustration of the formation of self-assembled HA–QDs–MEL conjugate in aqueous solution. QDs and MEL were attached to the backbone of HA *via* amidization using EDC/NHS reagents.

of T_n, and m_0 (μg) is the total amount of MEL in HA–QDs–MEL nanoparticles.

2.5. Cell culture evaluation

The human breast cancer (MDA-MB-453) cell lines and normal breast cell (HBL-100) cell lines were purchased from Wuhan Boster Company (Wuhan, China). By cultured at 37 °C in a humidified atmosphere containing 5% CO_2 in DMEM medium supplemented with 10% fetal bovine serum, 100 U/mL penicillin-streptomycin, and 0.5% amphotericin, several different procedures were employed.

A) To evaluate the cytotoxicity, MTT assays were conducted following the standard protocol (Homma et al., 2009). Cells were plated at a density of 1×10^4 cells/well in 96-well plates and subsequently incubated for 48 h with various concentrations of MEL, QDs, HA-QDs, MEL and HA–QDs–MEL nanoparticles. Each sample was tested in 5 parallel wells. After infection, the wells were replaced and the cells were washed three times with PBS (pH = 7.4) before addition of 180 μL of fresh medium and 20 μL of MTT solution (5 mg/mL). After incubation for another 4 h, the medium containing MTT was carefully removed and 150 μL of DMSO was added to dissolve the crystals remained inside the cells. The optical density (OD) was measured at 570 nm with a multi-well plate reader (Bio-Rad Laboratories B.V., Veenendaal, Netherlands). The cell viability was calculated by the following equation.

$$\text{Viable cells } (\%) = \frac{\text{OD}_{\text{treated}}}{\text{OD}_{\text{control}}} \times 100\% \quad (2)$$

where $\text{OD}_{\text{treated}}$ was obtained in the presence of samples. $\text{OD}_{\text{control}}$ was obtained with the control medium.

B) To study the intracellular localization, cells were seeded in 96-well plates at a density of 1×10^5 cells/mL and allowed to adhere for 24 h. Then, the culture medium was replaced by other culture mediums containing 1 μg/mL of QDs (excitation at 380 nm and emission at 580 nm), HA-QDs and HA–QDs–MEL, respectively. The culture medium set as the control. After 24 h of incubation, the drug-containing solutions were removed and

250 nM Lysotracker Green DND-26 (Sigma–Aldrich, USA, excitation at 504 nm and emission at 511 nm) was added, in which the cells were incubated for another 20 min. Then, 5 μg/mL of Hoechst 33342 (Ex 345 nm, Em 478 nm) was added for 10 min. At the end of incubation, the cells were washed three times with PBS (pH = 7.4) and fixed with a 2% paraformaldehyde solution for 15 min at 4 °C. The intracellular localization of samples was observed using a confocal fluorescence microscope (Nikon Eclipse C1, Japan).

C) To understand the effect of receptor inhibition on cellular Uptake, cells were pre-incubated with 10 μg/mL, 20 μg/mL, and 40 μg/mL of HA for 30 min at 37 °C. 1 μg/mL of HA–QDs–MEL solution was added thereafter to co-incubate for 1 h. Cells were washed, harvested, and observed by confocal fluorescence as described above.

3. Results and discussion

Gratifyingly, the HA–QDs–MEL polymer–drug conjugate was synthesized by covalently binding QDs and MEL to the backbone of HA *via* amidization (Fig. 1). The yield of the HA–QDs–MEL conjugate was about 77%, the drug loading was 19.8% and the Zeta potential was 0.75 ± 0.01 mV with a diameter of 115 ± 2.3 nm. The conjugate can form self-assembled nanoparticles in aqueous solutions, providing a hydrophobic inner core as the container of MEL and the hydrophilic HA and QDs shell as the targeting moiety of tumor tissues. It has an ideal drug release profile because of the easy degradation of the HA backbone and an ideal tracer *in vitro* to tumor cell under the effect of QDs and HA (Fig. 1).

3.1. Characterization

3.1.1. FT-IR

The FT-IR spectra of HA, QDs, MEL, and HA–QDs–MEL were shown in Fig. 2. The band at 3387 cm^{-1} in the spectra of HA corresponds to the OH group of HA. The peak at 2926 cm^{-1} is caused by the telescopic vibration of C-H bond in —CH_2— moieties. The band at 1609 cm^{-1} is the characteristic peak of amide. The absorptions at 3334 and 3288 cm^{-1} in the FT-IR spectra of QDs are belong to amino acid (L-cys). The bands at 1609 cm^{-1}, 1581 cm^{-1}, 1516 cm^{-1}, and 1450 cm^{-1} in the FT-IR spectra of MEL are the characteristic absorption peaks of benzene, which are from MEL. Furthermore, the bands at 1689 cm^{-1} and 1558 cm^{-1} in the FT-IR spectra of HA–QDs–MEL are attributed to the amides of HA–QDs–MEL. The characteristic peaks of HA, QDs and MEL were also observed in the spectra. These results indicated that HA–QDs–MEL conjugate was successfully synthesized.

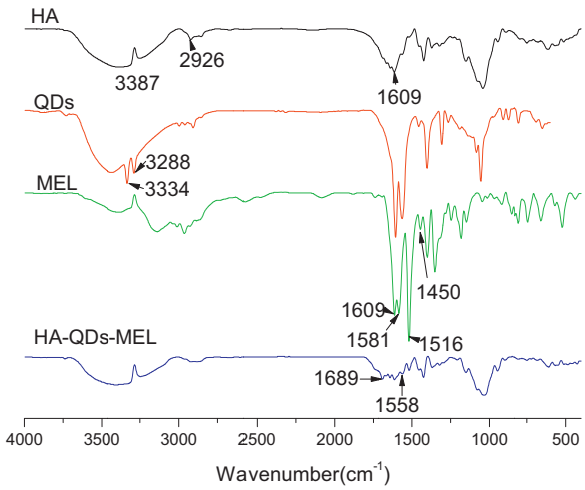

Fig. 2. FT-IR spectra of HA, QDs, MEL, and HA–QDs–MEL.

3.1.2. XRD, ^1H NMR and UV–vis

The XRD spectra of QDs were described in Fig. 3A. From the spectra, at 18.8, 28.4 and 40.5 were attributed to the signal of Cd. Similarly, the ^1H NMR spectra of HA–QDs–MEL was reported in Fig. 3B. The signals ranging from 2.87 to 4.09 ppm is attributed to the protons in the sugar ring of HA, while the peak at 4.50 ppm belongs to the proton of hydrogen attributed to the sugar end group. The signal at 5.09 ppm corresponds to the —NH_2 group and the signal at 1.07 ppm belongs to the —SH group of L-cys. The signals at 6.63 ppm and 6.90 ppm are the characteristic peaks of phenyl rings. The signal at 7.28 ppm is identified to the N—H bonds of amides. Moreover, the UV–vis spectra of HA, QDs and HA–QDs–MEL was shown in Fig. 3C. The characteristic peak of phenyl rings at 260 nm was also observed. All these indicated that the polymer–drug conjugate HA–QDs–MEL was favorably constructed.

3.2. In vitro drug release

The drug release profiles of the HA–QDs–MEL conjugate in an acidic (pH = 5.8), a neutral (pH = 7.0), and a weak alkaline (pH = 7.4) environment either with or without hyaluronidase were explored (Fig. 4). The accumulative release rates were initially fast for all groups, and then became slower as time progressed with a pH-enzyme sensitive release property. With hyaluronidase, the maximum accumulative release rate was 72% (pH = 5.8), 32% (pH = 7.0) and 22% (pH = 7.4), respectively. There were significant differences ($P < 0.05$) between the groups with pH = 5.8 and pH = 7.0, and ($P < 0.05$) between the groups with pH = 5.8 and

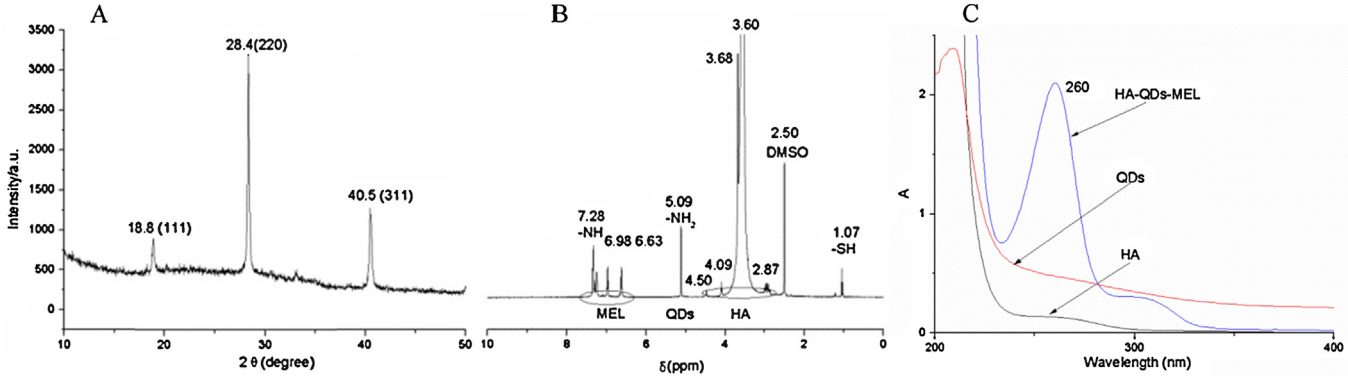

Fig. 3. (A) XRD of QDs, (B) ^1H NMR spectra of HA–QDs–MEL (600 MHz, DMSO-d_6, δ_{sol} = 2.50 ppm). (C) UV–vis of HA, QDs, and HA–QDs–MEL.

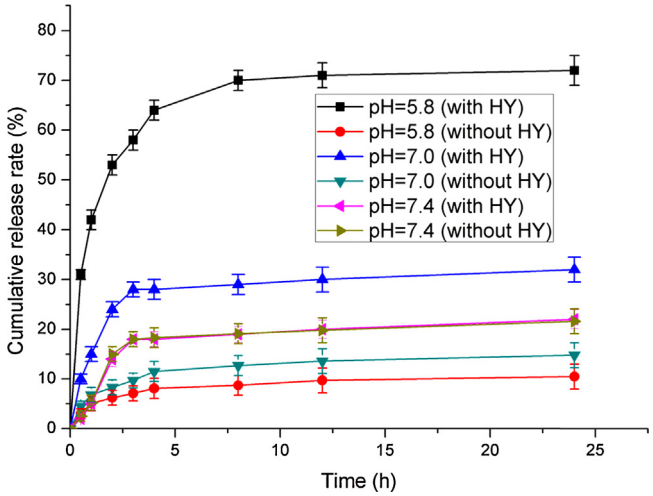

Fig. 4. *In vitro* drug release profiles of HA–QDs–MEL conjugate in PBS with various pH values (5.8, 7.0, and 7.4) at 37 ± 0.5 °C. The error bar represents the standard deviation (n = 5). HY refers to hyaluronidase.

pH = 7.4. However, there was no significant difference (P > 0.05) among the samples without hyaluronidase.

These release profiles may be the results of the synergistic effects of HA–QDs–MEL conjugate. First, HA can be naturally degraded in the organisms *via* a complex enzymatic digestion mechanism. This unique degradation process is mainly regulated by the specific enzyme known as hyaluronidase, which cleaves the —*N*-acetyl-d-glucosaminidic linkages in the HA backbone. Moreover, the hyaluronidase has better digestion ability under acidic conditions, particularly when the pH value is around 5.5–6.0; it almost lost the function of enzymatic hydrolysis under neutral to alkaline environment (Moghimi & Szebeni, 2003). Second, Melphalan (MEL), a chemotherapy drug, is the nitrogen mustard alkylating agent derived from mechlorethamine, which can improve the drug release by promoting the enzyme recognition of the conjugate. As a result, the HA–QDs–MEL conjugate had a very good performance of drug release in tumor microenvironment due to the natural recognition and biodegradability of HA by hyaluronidase and the promoted recognition ability by MEL. The faster the protective HA shell around the conjugated drug is degraded, the quicker the drug is released. The HA–QDs–MEL conjugate has advantages with regard to cellular internalization of tumor cells. The normal tissue is weakly alkaline (pH = 7.4), and the tumor tissues and their surroundings are quite acidic (pH value is around 4.5–6.0) with high expression of CD44 receptors, which can enforce HA-conjugate toward the tumor sites. Hence, the HA–QDs–MEL conjugate was stable in the blood and normal tissues with a pH of about 7.4, whereas the drug releases in the tumor tissues due to the hyaluronidase-catalyzed degradation under acidic physiologic conditions (pH value is around 5.8). The released drug and particles were then internalized into the tumor cells together with HA. This drug delivery system HA–QDs–MEL conjugate showed excellent drug release properties and may be a prospective candidate for cancer chemotherapy with very high selectivity and low adverse effects on normal tissues.

3.3. *In vitro* cell evaluation

3.3.1. *Cytotoxicity of the HA–QDs–MEL conjugate*

The *in vitro* cytotoxicities of MEL, HA-QDs, HA–QDs–MEL, and $HA_{(d)}$–QDs–MEL, which were the degradation products of HA–QDs–MEL (MW = 438,000 determined by gel permeation chromatography), were evaluated using MTT assay, as shown in Fig. 5. It was found that HA-QDs almost had no inhibition effect on both two kinds of cells. MEL and HA–QDs–MEL can inhibit the growth of human breast cancer cell lines (MDA-MB-453) with a dose-dependent effect. The cell viability of MEL group (25%) was higher than HA–QDs–MEL (19%) with significant difference (P < 0.05) (Fig. 5A). In contrast, the cell viability of normal breast cell lines (HBL-100) by HA–QDs–MEL was higher than that by MEL even at the largest dose with no significant difference (Fig. 5B). Interestingly, the cell viabilities of $HA_{(d)}$–QDs–MEL were lower than those of HA–QDs–MEL with the same concentration. These findings indicated that the HA–QDs–MEL conjugate had a higher cytotoxicity to tumor cell and a lower cytotoxicity to normal cells, compared with free MEL. This might be due to the selective toxicity of HA–QDs–MEL toward human breast cancer (MDA-MB-453) cell lines. Over-expression of CD44 receptor on MDA-MB-453 cells can promote cellular internalization after binding to HA. Once the covalent bond is cleaved by intracellular enzymes including hyaluronidase, HA-conjugates in the cells would release drug. Moreover, the low MW of HA maybe makes the conjugate transfer

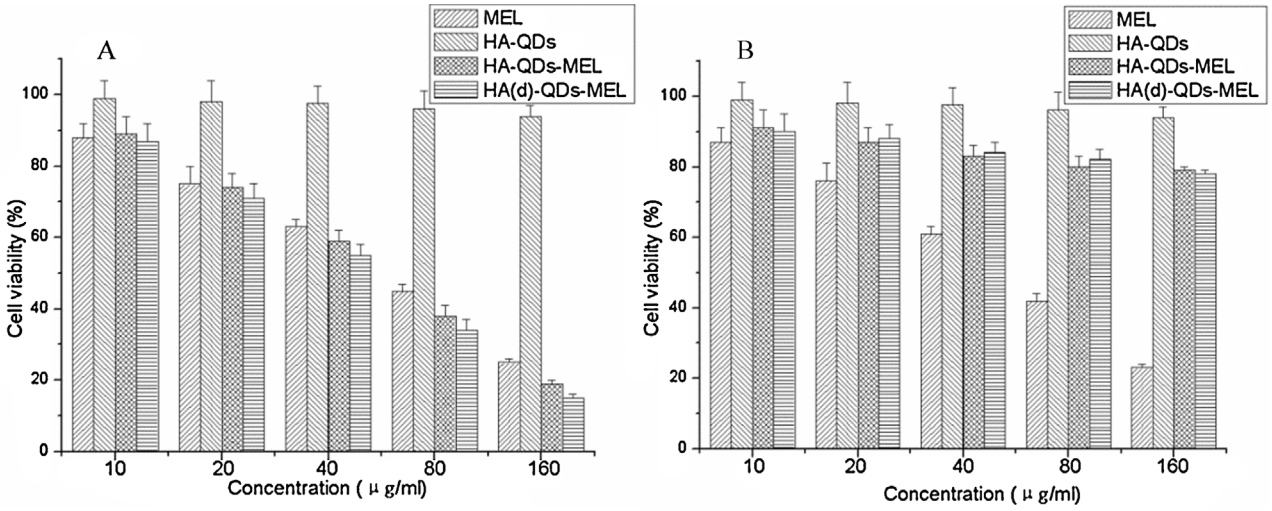

Fig. 5. Cytotoxicity test of cells with MEL, HA-QDs, HA–QDs–MEL, and $HA_{(d)}$–QDs–MEL (the degradation products of HA–QDs–MEL (MW = 43,8000 determined by gel permeation chromatography)) in different dosages over 48 h. (A) Cytotoxicity to the human breast cancer cell lines (MDA-MB-453). (B) Cytotoxicity to the normal breast cell lines (HBL-100). The error bar represents the standard deviation (n = 5).

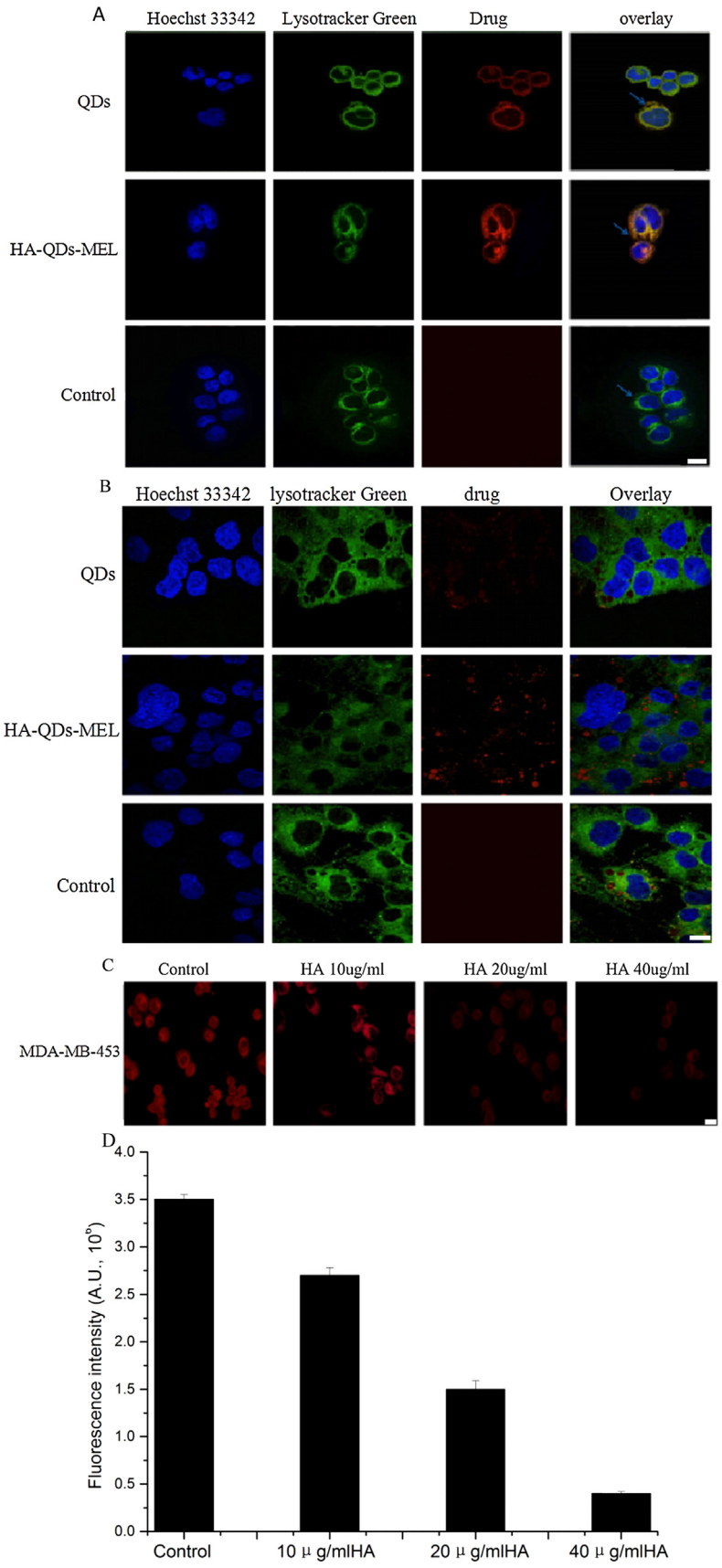

Fig. 6. (A) The intracellular localization of QDs and HA–QDs–MEL in the human breast cancer cells for 24 h. (B) The intracellular localization of QDs and HA–QDs–MEL in the normal human breast cells for 24 h. (C) The pictures of HA–QDs–MEL internalization with HA as an inhibitor. (D) The fluorescence intensity of HA–QDs–MEL with different concentrations of HA.

into cells easily. It was also reported that the HA with low MW is helpful for treating cancers (Carole et al., 2011).

3.3.2. Cellular uptake of the conjugate

To study the receptor-mediated cellular uptake, the HA–QDs–MEL conjugate was incubated with the human breast cancer cell lines (MDA-MB-453) and the normal breast cell lines (HBL-100). The cells, fixed at pre-determined time points, were then analyzed using the confocal fluorescent microscope. The human breast cancer cell has been demonstrated to over-express CD44 on their surfaces, compared to normal cells including the normal breast cell lines. As shown in Fig. 6, fluorescent signals were observed in the cancer cells that were treated with conjugate for 24 h. On the other hand, HA–QDs–MEL conjugate hardly moved into the normal breast cell lines. The signals of the normal breast cell lines treated with conjugate were much weaker than those of the cancer cells.

These findings indicated that the HA–QDs–MEL conjugate can self-assemble into nanoparticles in aqueous media with MEL entrapped inside the hydrophilic HA outer shell with an appropriate diameter for drug to release. The conjugate exhibited good drug release performance and cell cytotoxicity with high selectivity under simulated tumor microenvironment conditions.

4. Conclusion

A HA–QDs–MEL conjugate was synthesized and characterized by XRD, FT-IR spectroscopy, ^{1}H NMR, UV–vis, and DLS. The conjugate can form nanoparticles in an aqueous solution with an appropriate diameter and Zeta potential for active targeting. The drug release profiles were pH sensitive. The drug release rate (72%) was much faster under acidic conditions (pH = 5.8), which simulate the microenvironment of the cancer cells or tissues, than that (22%) under slightly basic conditions (pH = 7.4), imitating the microenvironment of the normal cells or tissues in the presence of hyaluronidase with significant difference ($P < 0.05$). Cytotoxicity test showed that the HA–QDs–MEL conjugate had a stronger cytotoxicity against human breast cancer cell lines (MDA-MB-453) than free MEL did, with significant difference ($P < 0.05$). Besides, the HA–QDs–MEL conjugate had a lower toxicity to the normal breast cell lines (HBL-100) compared with free MEL. These findings indicated that the novel HA–QDs–MEL conjugate can not only enhance the anti-tumor effect of MEL, but also minimize the undesirable side effects on normal cells, leading to a promising targeting specific drug delivery system for tumor therapy.

Declaration of conflicting interests

The authors declare no conflict of interest.

Acknowledgements

The authors wish to thank the National Natural Science Foundation of China [grant number: 51473130], the Innovation Research Fund of Undergraduate Special Project [grant number: 136620004], the Research Fund of Innovation Projects for Graduate Students [grant number: 2014-zy-221], and the National College Students Innovation Programs [grant number: 20141049720005] for their financial supports.

References

Akima, K., Ito, H., Iwata, Y., Matsuo, K., Watari, N., & Yanagi, M. (1996). Evaluation of antitumor activities of hyaluronate binding antitumor drugs: Synthesis, characterization and antitumor activity. *Journal of Drug Targeting*, *4*, 1–8.

Aruffo, A., Stamenkovic, I., Melnick, M., Underhill, C., & Seed, B. (1990). CD44 is the principal cell surface receptor for hyaluronate. *Cell*, *61*, 1303–1313.

Baracu, N. I., Balaban, A. T., & Wilman, D. E. (1990). *The chemistry of antitumor agents*. Glasgow, London: Blackie.

Carole, E. S., Guy, Z., Corinne, H., & Thierry, F. V. (2011). Chemical modifications of hyaluronic acid for the synthesis of derivatives for a broad range of biomedical applications. *Carbohydrate Polymers*, *85*, 469–489.

Carole, E. S., Guy, Z., Corinne, H., & Thierry, F. V. (2012). Improvement of hyaluronic acid enzymatic stability by the grafting of amino-acids. *Carbohydrate Polymers*, *87*, 2211–2216.

Fermeglia, M., Ferrone, M., Lodi, A., & Pricl, S. (2003). Host–guest inclusion complexes between anticancer drugs and b-cyclodextrin: Computational studies. *Carbohydrate Polymers*, *53*, 15–44.

Girish, K. S., & Kemparaju, K. (2007). The magic glue hyaluronan and its eraser hyaluronidase: A biological overview. *Life Sciences*, *80*, 1921–1943.

Goodarzi, N., Varshochian, R., Kamalinia, G., Atyabi, F., & Dinarvand, R. (2013). A review of polysaccharide cytotoxic drug conjugates for cancer therapy. *Carbohydrate Polymers*, *92*, 1280–1293.

Hansson, J., Lewensohn, R., Ringborg, U., & Nilsson, B. (1987). Formation and removal of DNA cross-links induced by melphalan and nitrogen mustard in relation to drug-induced cytotoxicity in human melanoma cells. *Cancer Research*, *47*, 2631–2637.

Hauck, T. S., Anderson, R. E., Fischer, H. C., Newbigging, S., & Chan, W. C. W. (2010). In vivo quantum-dot toxicity assessment. *Small*, *6*, 138–144.

Homma, A., Sato, H., Okamachi, A., Emura, T., Ishizawa, T., & Kato, T. (2009). Novel hyaluronic acid–methotrexate conjugates for osteoarthritis treatment. *Bioorganic and Medicinal Chemistry*, *17*, 4647–4656.

Hridyesh, K., Rohit, S., & Dutta, P. K. (2013). Highly luminescent chitosan-l-cysteine functionalized CdTe quantum dots film: Synthesis and characterization. *Carbohydrate Polymers*, *97*, 327–334.

Jedrzejas, M. J., & Stern, R. (2005). Structures of vertebrate hyaluronidases and their unique enzymatic mechanism of hydrolysis. *Proteins*, *61*, 227–238.

Khandare, J., & Minko, T. (2006). Polymer–drug conjugates: Progress in polymeric prodrugs. *Progress in Polymer Science*, *2006*, 359–397.

Laura, M., Marco, B., & Luisa, R. (2014). Amphiphilic hyaluronic acid derivatives toward the design of micelles for the sustained delivery of hydrophobic drugs. *Carbohydrate Polymers*, *102*, 110–116.

Li, Y. L., Duan, X., & Jing, L. H. (2011). Quantum dot-antisense oligonucleotide conjugates for multifunctional gene transfection, mRNA regulation, and tracking of biological processes. *Biomaterials*, *32*, 1923–1931.

Li, D., Lu, B., Huang, Z., Xu, P., Zheng, H., Yin, Y., et al. (2014). A novel melphalan polymeric prodrug: Preparation and property study. *Carbohydrate Polymers*, *111*, 928–935.

Lu, B., Huang, D., Zheng, H., Huang, Z., Xu, P., Xu, H., et al. (2013). Preparation, characterization, and in vitro efficacy of O-carboxymethyl chitosan conjugate of melphalan. *Carbohydrate Polymers*, *98*, 36–42, 2013.

Luo, Y., & Prestwich, G. (1999). Synthesis and selective cytotoxicity of a hyaluronic acid-antitumor bioconjugate. *Bioconjugate Chemistry*, *10*, 755–763.

Luo, Y., Ziebell, M., & Prestwich, G. (2000). A hyaluronic acid–Taxol antitumor bioconjugate targeted to cancer cells. *Biomacromolecules*, *1*, 208–218.

Majoros, I. J., Thomas, T. P., Mehta, C. B., & Baker, J. R. (2005). Poly(amidoamine) dendrimer-based multifunctional engineered nanodevice for cancer therapy. *Journal of Medicinal Chemistry*, *48*, 5892–5899.

Maze, R., Carney, J. P., Kelley, M. R., Glassner, B. J., Williams, D. A., & Samson, L. (1996). Increasing DNA repair methyltransferase levels via bone marrow stem cell transduction rescues mice from the toxic effects of 1,3-bis (2-chloroethyl)-1-nitrosourea, a chemotherapeutic alkylating agent. *Proceedings of the National Academy of Sciences USA*, *93*, 206–210.

Moghimi, S. M., & Szebeni, J. (2003). Stealth liposomes and long circulating nanoparticles: Critical issues in pharmacokinetics, opsonization and protein-binding properties. *Progress in Lipid Research*, *42*, 463–478.

Moghimi, S. M., Hunter, A. C., & Murry, J. C. (2005). Nanomedicine: Current status and future prospects. *FASEB Journal*, *19*, 311–330.

Patri, A. K., Majoros, I., & Baker, J. R. (2002). Dendritic polymer macromolecular carriers for drug delivery. *Current Opinion in Chemical Biology*, *6*, 466–471.

Pouyani, T., & Prestwich, G. (1994). Functionalized derivatives of hyaluronic acid oligosaccharides: Drug carriers and novel biomaterials. *Bioconjugate Chemistry*, *5*, 339–347.

Shan, L. L., Cui, S. S., Du, C. L., Wan, S. N., Qian, Z. Y., Achilefu, S., et al. (2012). A paclitaxel-conjugated adenovirus vector for targeted drug delivery for tumor therapy. *Biomaterials*, *33*, 146–162.

Shen, Y., Li, Q., Tu, J., & Zhu, J. (2009). Synthesis and characterization of low molecular weight hyaluronic acid-based cationic micelles for efficient siRNA delivery. *Carbohydrate Polymers*, *77*, 95–104.

Sonia, A. Q., Ana, G., & Carmen, R. L. (2011). Microspheres loaded with polysaccharide nanoparticles for pulmonary delivery: Preparation, structure and surface analysis. *Carbohydrate Polymers*, *86*, 25–34.

Suzukake, K., Vistica, B. P., & Vistica, D. T. (1983). Dechlorination of L-phenylalanine mustard by sensitive and resistant tumor cells and its relationship to intracellular glutathione content. *Biochemical Pharmacology*, *32*, 165–167.

Taetz, S., Bochot, A., Surace, C., Arpicco, S., Renoir, J. M., & Schaefer, U. F. (2009). Hyaluronic acid-modified DOTAP/DOPE liposomes for the targeted delivery of anti-telomerase siRNA to CD44-expressing lung cancer cells. *Oligonucleotides*, *19*, 103–116.

Wang, Y. Q., & Chen, L. X. (2011). Quantum dots, lighting up the research and development of nanomedicine. *Nanomedicine: Nanotechnology, Biology, and Medicine*, *7*, 385–402.

Xin, D., Wang, Y., & Xiang, J. (2010). The use of amino acid linkers in the conjugation of paclitaxel with hyaluronic acid as drug delivery system: Synthesis, self-assembled property, drug release, and in vitro efficiency. *Pharmaceutical Research*, *27*, 380–389.

Zhao, Y. L., Liu, S., & Li, Y. P. (2010). Synthesis and grafting of folate-PEG-PAMAM conjugates onto quantum dots for selective targeting of folate-receptor-positive tumor cells. *Journal of Colloid and Interface Science*, *350*, 44–50.